

THE ANALYSIS OF FEM RESULTS CONVERGENCE IN MODELLING PIEZOELECTRIC ACTIVE SHELL STRUCTURES

UDC 624.04+531:519.6

Summary

The field of active/adaptive structures has been the subject of intense interest over the past couple of decades. The progress in this research field strongly depends on the availability of adequate and reliable modelling tools. Regarding structural analysis in general, the finite element method (FEM) has imposed itself as the method of choice for modelling and simulation. Piezoelectric active structures are characterized by strong enough coupling between the mechanical field and the electric field, which is further used for the realization of active structural behaviour. The descriptions of the mechanical and electrical field as well as their coupling significantly affect the convergence of the FEM results with mesh refinement, which may proceed in a trend different to what is commonly expected when FEM is applied to purely mechanical problems. The paper considers this aspect by using two quadratic shell type finite elements developed for modelling piezoelectric composite laminates. Both full and uniformly reduced integration techniques are taken into consideration in a set of examples involving composite laminates with active piezoelectric layers.

Key words: FEM, solution convergence, active structures, shell, piezoelectric actuation

1. Introduction

Significant attention has been given to active/adaptive structures over the past two decades. It is their intrinsic property to mimic the behaviour of natural systems that serves as an impetus for researchers to steadily broaden the area of application of adaptive systems. The general idea consists of the use of advanced multifunctional materials in order to design and integrate active elements, i.e. sensors and actuators, into structures and thus provide the means for their active behaviour. Many researchers have focused their work on possible applications, whereas the others have turned their attention to the need for reliable modelling and simulation of active structures' behaviour.

The finite element method (FEM) has established itself as the method of choice for the problems in the field of structural analysis. The application of the FEM in the field of mechanical problems has been thoroughly studied in the past 50 years. This involves techniques for obtaining reliable, high quality solutions. The FEM is also widely used in the field of

coupled-field problems, such as electro-mechanical problems characteristic of active structures with piezoelectric active elements. Since a reliable simulation is supposed to provide an easier, faster and less expensive development of adaptive structures, this paper looks at the aspect of FEM results convergence when thin-walled piezoelectric structures are considered. The aspect is important as a different trend in the development of FEM results with mesh refinement can occur in many coupled-field cases compared to purely mechanical problems. This paper focused on thin-walled structures notoriously famous for locking effects, such as shear or membrane locking, that significantly affect the convergence of the mechanical field [1]. A number of authors have offered various techniques to improve the convergence of FEM results in such cases. Among the solutions are the addition of bubble/incompatible modes [2], discrete shear gap and assumed natural strain approach [3], selectively [4] and uniformly [5] reduced integration, mixed interpolation of tensorial components [6], etc. Some authors have pointed out that the solutions relying on hybrid formulations are less sensitive to mesh distortion [7, 8]. Liu *et al* [9] have combined the displacement-based FEM formulation with a strain smoothing technique of mesh-free methods to produce the smoothed finite element method, whereby the smoothing technique is developed based on the Hu–Washizu three-field variational principle. The amount of efforts invested in resolving the problem demonstrates the interest of the research community to improve this aspect of the FEM modelling of adaptive structures.

This paper points out the difference between the FEM models involving purely mechanical field and those related to coupled electro-mechanical field with piezoelectric actuation. It further discusses how this difference affects the convergence of FEM results with mesh refinement. The purely mechanical examples from [10] have been modified to include the piezoelectric (electro-mechanical) coupling in order to be considered in this paper. For the FEM modelling, two different shell type finite elements, developed for thin-walled active structures, have been used.

2. Material architecture, mechanical and electrical field and their coupling

Thin-walled active structures with piezoelectric patches as active elements imply the use of composite material architecture. Considering the material architecture across the thickness of the structure, one may notice that it consists of multiple types of layers involving passive and active (piezoelectric) layers. Passive layers are load-carrying layers, whereas piezoelectric layers serve as active elements, i.e. sensors and actuators, through the electro-mechanical coupling. Even the passive material alone is quite often a fibre-reinforced composite laminate. This means that several layers of fibre-reinforced composite material are bonded together to form a laminate of desired thickness, sequence of layers (orientation of fibres), choice of constituent materials (fibres and matrix), etc. The active piezoelectric patches are either embedded into such a laminate or bonded onto the outer surfaces, thus providing the means for active behaviour of the structure. Finally, sensors and actuators are coupled to each other by means of a controller, which implements the strategy of structural behaviour, and the structure becomes adaptive (Fig. 1).



Fig. 1 Composite material architecture of an adaptive car-roof

For better understanding of the aspects arising in the FEM modelling of coupled electro-mechanical problems, it would be worthwhile to give the basic equations that describe the mechanical field (strains, stresses), electrical field (electric field, potential) and their coupling.

Efficient modelling of thin-walled structures is driven by the recognition that the nature of the global behaviour of such structures allows condensation of the complex 3D-field to the essential ingredients of the structural response described by a 2D approach. A general shape assumes arbitrarily curved structures and, regardless of the applied loads, both membrane and flexural strains are induced in such a structure. Furthermore, thin-walled structures made of composite laminates require 2D-theories with transverse shear strains and stresses included for adequate modelling. The simplest and most frequently used theory is the First-order Shear Deformation Theory (FSDT), which is based on the Mindlin-Reissner kinematical assumptions that imply constant transverse shear strains and stresses across the thickness of the structure [11].

Within the framework of the FEM, the strain field of a shell element based on the aforementioned kinematical assumptions is given in the following general form:

$$\{\boldsymbol{\varepsilon}\} = \begin{Bmatrix} \{\boldsymbol{\varepsilon}_{mf}\} \\ \text{---} \\ \{\boldsymbol{\varepsilon}_s\} \end{Bmatrix} = \begin{bmatrix} [\mathbf{B}_{mf}] \\ \text{---} \\ [\mathbf{B}_s] \end{bmatrix} \{\mathbf{d}_e\} = [\mathbf{B}_u] \{\mathbf{d}_e\}, \quad (1)$$

where $\{\boldsymbol{\varepsilon}_{mf}\}$ and $\{\boldsymbol{\varepsilon}_s\}$ are the membrane-flexural (in-plane) and transverse shear strains, respectively, $[\mathbf{B}_{mf}]$ and $[\mathbf{B}_s]$ are corresponding strain-displacement matrices and can be summarized into the element strain-displacement matrix $[\mathbf{B}_u]$, and, finally, $\{\mathbf{d}_e\}$ are the element nodal displacements. For more details on the definition of the strain field, an interested reader is referred to [11].

Regarding the electric field within the active layers, it is assumed that the piezolayers are polarized in the thickness direction, with a constant value of electric potential over the electrodes bonded onto the outer surfaces of the piezolayer. The actual distribution of the electric field and electric potential across the thickness of the piezolayer can be deduced from Gauss's law for dielectrics and it depends on the kinematics of deformation [11]. One may demonstrate that a first-order 2D theory (linear function for the in-plane displacements across the thickness) results in the quadratic distribution of electric potential and linear distribution of electric field. However, the conducted analyses [12, 13] have also demonstrated that a constant approximation for the electric field, typically used by a great number of researchers in this field, is quite satisfying for the current class of piezoelectric materials and rather thin piezopatches. It results in a very simple equation for the electric field:

$$E_k = -\frac{\Phi_k}{h_k}, \quad (2)$$

where Φ_k is the difference of electric potentials between the electrodes of the k^{th} piezolayer in the laminate (i.e. this is the k^{th} electrical degree of freedom of the element) and h_k is the thickness of the piezolayer.

The coupling between the mechanical and electrical field is described by means of the piezoelectric material constitutive equation. The form of this equation depends on the choice of independent variables [14] and, in the framework of the displacement-based FEM, those are the mechanical displacements and the electric voltages. The corresponding piezoelectric material constitutive equation reads:

$$\begin{aligned}\{\sigma\} &= [C^E]\{\varepsilon\} - [e]\{E\} \\ \{D\} &= [e]\{\varepsilon\} + [d^e]\{E\}\end{aligned}\quad (3)$$

where $\{\sigma\}$ is the mechanical stress in vector (Voigt) notation, $\{D\}$ is the electric displacement vector, $[C^E]$ is the material Hook's matrix at constant electric field E , $[d^e]$ is the dielectric permittivity matrix at constant ε , and $[e]$ is the piezoelectric coupling matrix. It should be emphasized that the considered active elements operate using the piezoelectric "e₃₁-effect", thus coupling the in-plane strains to the perpendicularly applied electric field.

3. Locking phenomena and influence on FEM results convergence

The considered type of problem involves both the mechanical and electrical field with the two-way coupling between them, as given by Eq. (3). The description of the electrical field is rather straightforward (Eq. (2)) and it does not produce any numerical difficulties when convergence check is performed by means of FE mesh refinement. However, it is coupled to the mechanical field which is, on the other hand, notorious for problems denoted as locking phenomena.

Locking phenomena represent an intrinsic problem of the finite elements which, in their application, encounter constrained field problems. Considering thin-walled structures with high slenderness, they are known to deform in such a manner that transverse shear strains are not involved in the deformational behaviour. Hence, in this type of deformation, the transverse shear strain and stress fields are constrained. Similarly, pure bending occurs without membrane strains. However, typical isoparametric shell formulations, based on the Mindlin-Reissner kinematical assumptions, result in elements that are incapable of correctly representing such deformational states. The consequence is the presence of parasitic strains and stresses in the FEM results, whereas they are not a part of the considered actual physical regimes, and the model predicts stiffer behaviour compared to the real structural behaviour. The above mentioned issues are denoted as shear and membrane locking, respectively.

According to Prathap [1], a variationally correct solution for the aforementioned issues requires the introduction of the paradigms of field-consistency and variational correctness. He could successfully demonstrate those postulates and adequate solutions for simpler types of finite elements, such as beams or plates. But Prathap has also concluded that the class of degenerate shell elements exhibits high level of complexity originating from multiple mappings between coordinate systems, which prohibit tracking of inconsistent constrained fields and their reconstitution in a variationally correct manner. Hence, at this stage of development, simpler techniques, but which offer no guarantee of variational correctness (actually, they were deemed as "variational crime" by Prathap), are to be applied. Some of those have been mentioned in the introduction to the paper. Prathap points out the uniformly reduced integration as one of the simplest and most effective techniques for this purpose, when arbitrarily shaped biquadratic degenerate shell element is used.

Hence, in the considered coupled-field problem, the FEM description of the mechanical field is accompanied by the aforementioned issues that affect the quality of the result convergence, whereas the electrical field model is relatively simple and not essentially influenced by the FEM mesh refinement. However, the two fields are coupled to each other, which is the basic ingredient of the active behaviour of piezoelectric structures. In the following, a set of examples will be considered in order to investigate the convergence of the FEM results with mesh refinement for the coupled electro-mechanical field. Both full and uniformly reduced integration techniques will be considered.

4. Analysis of FEM results convergence presented on examples

The examples involving purely mechanical cases considered in [10] are modified here to include active layers in order to investigate how the FEM results convergence proceeds when the coupled-field problems are handled. The structures considered in the examples are of shell type and are made of composite laminates composed of two types of layers – fibre reinforced composite (T300/976 graphite/epoxy) and piezoceramic (PZT G1195) layers. The elastic properties of the composite layers are considered to be transversely isotropic. They are given with respect to the material principles directions as: the Young moduli $Y_{11}=150$ GPa and $Y_{22}=9$ GPa, the shear modulus $G_{12}=7.1$ GPa and the Poisson coefficients $\nu_{12}=0.3$ and $\nu_{23}=0.3$. The piezoelectric layers are considered to have isotropic elastic properties with $Y=63$ GPa and $\nu=0.3$, while the piezoelectric constant is given as $e_{31}=2.286 \cdot 10^{-5}$ C/mm². Not specified piezoelectric constants are assumed to be equal to zero. In the examples, the dielectric constants are not required, as the electro-mechanical coupling is achieved through the inverse piezoelectric effect (actuator function) and only the mechanical quantities are of interest. This implies that the deformation of the considered structures is caused by the actuation of the piezolayers. In such a case, the static FEM equations of the coupled electro-mechanical field [11] reduce to the following equation:

$$[K_{uu}]\{d\} = -[K_{u\phi}]\{\phi\}, \quad (4)$$

where $[K_{uu}]$ is the mechanical stiffness matrix, $[K_{u\phi}]$ the piezoelectric coupling matrix, $\{d\}$ are the mechanical degrees of freedom and $\{\phi\}$ are the predefined electric voltages of the FEM model. The right-hand side of Eq. (4) defines piezoelectrically induced loads. In the considered examples, two oppositely polarized piezolayers are exposed to the same electric voltage. The position of piezolayers in the laminates is symmetric with respect to the laminate's reference plane. Hence, the actuation induces bending moments uniformly distributed along the edges of the piezolayers [11]. The sequence of layers will be specified in the following for each of the considered cases.

The analyses have been performed by means of the already developed [11] and verified [15, 16] full biquadratic *ACShell9* element (active composite shell with nine nodes) as well as the quadratic 8-node *Semi-Loof* shell element, originally developed by Irons [17] and extended by Gabbert et al. [18] to a piezoelectric laminate element. The *ACShell9* element is of Mindlin type and it is susceptible to both shear and membrane locking. The *Semi-Loof* element is based on the discrete Kirchhoff theory, which means that the transverse shear is not accounted for. Thus, only the membrane locking may act with the *Semi-Loof* element.

4.1 Clamped cylindrical shallow piezolaminated shell

In the first example, a cylindrical composite shell with the in-plane dimensions $a \times b = 254 \times 254$ mm and radius $R=10 \times a$ is considered (Fig. 3, left). The sequence of layers is defined with respect to the global x-axis (structure's reference direction). It is symmetric with the structure's mid-surface and reads $[PZT/30_2/0]_s$. This means that, across the thickness of the laminate, the orientation of unidirectional fibres with respect to the global x-axis is: PZT (no fibres), 30°, again 30° and 0° up to the mid-surface (Fig. 2) and further symmetric, i.e. 0°, 30°, 30°, PZT, so that altogether 8 layers render the laminate. The piezolayers are outer layers so that the maximal effect of their actuation (electric voltage 100 V) is achieved. The thickness of each composite layer is 0.138 mm and of each piezolayer 0.254 mm.

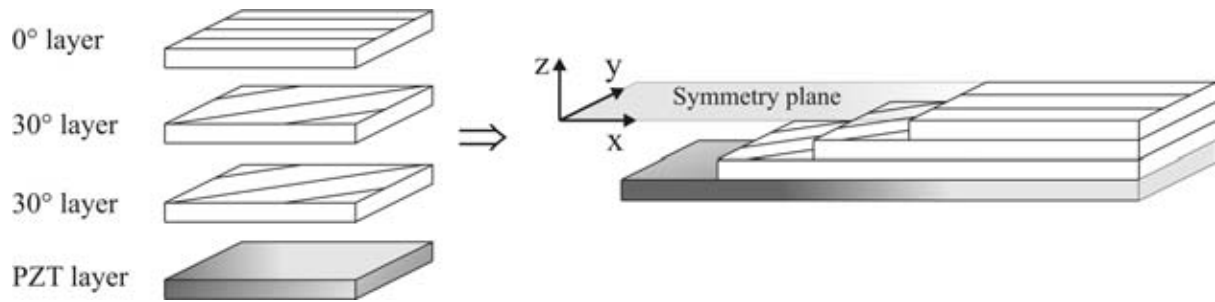


Fig. 2 Laminate setup for the sequence of layers [PZT/30₂/0]_s

As for the boundary conditions, one of the structure’s curved edges is clamped (Fig. 3, left). The structure has been discretized with four different meshes (Fig. 3, right) in order to investigate the FEM results convergence in this case of rather thin structure with the slenderness of approximately 190. The *ACShell9* element is used with both full (Gauss 3×3 integration rule) and uniformly reduced integration (Gauss 2×2 integration rule), while the *Semi-Loof* element is coded so that the full integration (3×3) is available only.

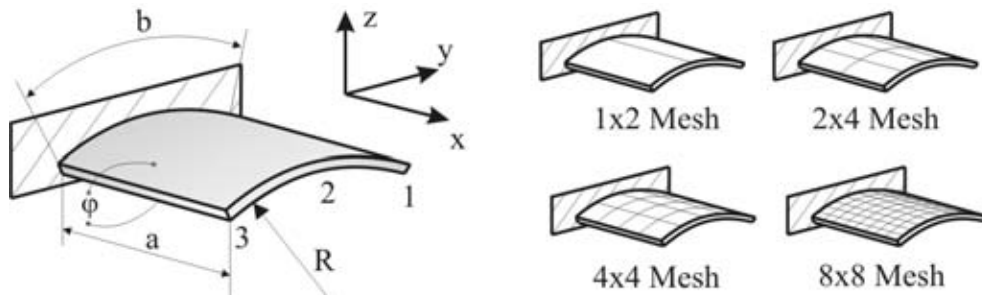


Fig. 3 Cylindrical active composite shell modelled by 4 FE meshes

Though symmetric, the stacking sequence of the laminate is ‘unbalanced’ due to 30° layers, which results in coupling in the structural behaviour not observed when isotropic materials are applied. Under the influence of the bending moments induced by the piezoelectric actuation, the shell structure bends and twists. To characterize such a deformation properly, the transverse deflection is observed at three points of the shell’s free edge. Those are the two end-points of the edge (points 1 and 3 in Fig. 3) and the mid-point (point 2 in Fig. 3). The obtained results are summarized in Table 1, where w_i/b , $i=1\div 3$, stands for the normalized transverse deflection of the three points, while *ACS9* and *SL* are abbreviations denoting *ACShell9* and *Semi-Loof* shell elements, respectively.

Table 1 Results at 3 characteristic points for 4 different FE meshes

Mesh	$(w_3/b) \times 10^{-3}$			$(w_2/b) \times 10^{-3}$			$(w_1/b) \times 10^{-3}$		
	<i>ACS9</i>	<i>ACS9</i>	<i>SL</i>	<i>ACS9</i>	<i>ACS9</i>	<i>SL</i>	<i>ACS9</i>	<i>ACS9</i>	<i>SL</i>
	3x3	2x2	3x3	3x3	2x2	3x3	3x3	2x2	3x3
1x2	-6.394	-6.299	-5.682	-4.241	-2.775	-3.380	-8.464	-10.385	-7.287
2x4	-6.840	-6.431	-6.163	-3.675	-3.359	-3.180	-10.439	-10.741	-10.193
4x4	-6.507	-6.423	-6.181	-3.603	-3.354	-3.343	-10.514	-10.762	-10.394
8x8	-6.450	-6.397	-6.347	-3.420	-3.367	-3.354	-10.732	-10.730	-10.686

A better overview of the obtained results can be provided in the form of diagrams. Figs. 4 and 5 offer such an overview. They give the normalized transverse deflection of the shell's free edge across the width. The coupling between bending and twisting of the shell is obvious from the results given in the diagrams. Fig. 4 gives the results obtained with the fully integrated *ACShell9* element. For the purpose of comparison, this diagram also includes the result for the finest (8×8) mesh with the reduced integrated element (denoted as (8×8)Mesh_RI). Fig. 5 gives the results yielded by the under-integrated *ACShell9* element.

It can be noticed that the values obtained by means of *ACShell9* element converge to the same result when the element is used with both full and reduced integration and those results are also in a quite good agreement with the results from the *Semi-Loof* shell element. In comparison to the convergence of the *ACShell9* element for the similar, only purely mechanical case reported in [10], a very interesting remark can be given. Namely, in the passive case, the convergence is monotone and it proceeds from below (full integration) or from above (reduced integration). This is actually the expected property of static FEM computations for the purely mechanical field. However, the results in Table 1 and Figs. 4 and

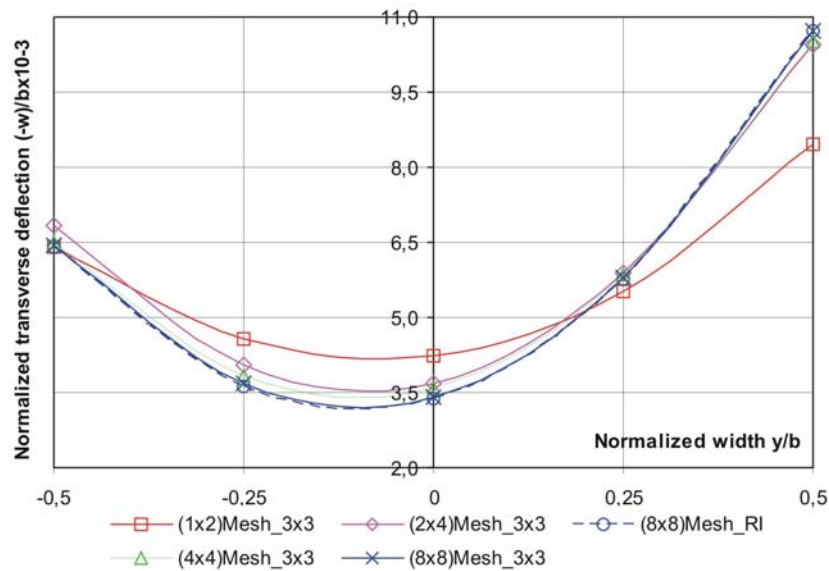


Fig. 4 Free edge transverse deflection – fully integrated *ACShell9* element

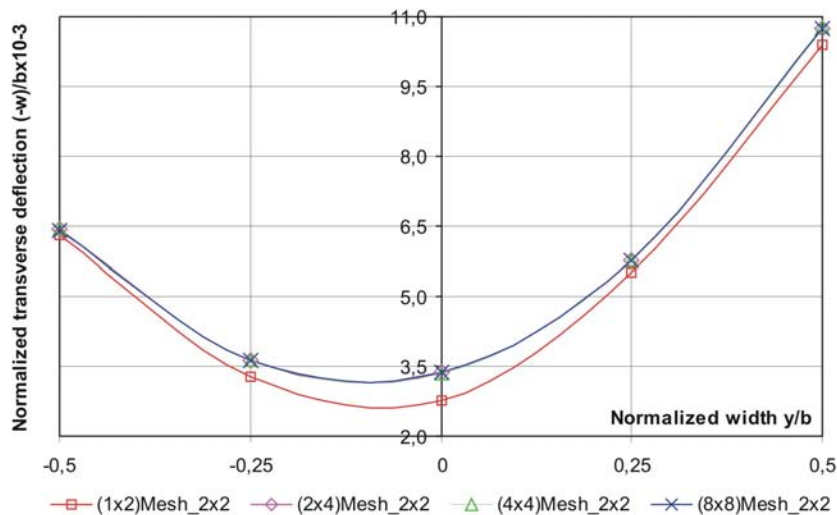


Fig. 5 Free edge transverse deflection – under-integrated *ACShell9* element

5 reveal that, in the coupled electro-mechanical case, the convergence proceeds in a non-monotone manner. This is the consequence of the fact that, with the mesh refinement, both sides of Eq. (4) are affected and they both converge to certain values, but not necessarily at the same rate. Another important remark is that the convergence rate of the reduced integrated *ACShell9* element is significantly higher, which is obvious from comparison of Figs. 4 and 5. The results obtained by the reduced integrated element for meshes (2×4), (4×4) and (8×8) are seen in Fig. 5 as almost congruent.

4.2 Simply supported piezolaminated arch

In the second example, a simply supported cylindrical arch with radius $R=100$ mm and width $b=62.8$ mm is considered (Fig. 6). The stacking sequence is symmetric $[PZT/45/-45/0]_s$ and balanced, thus resulting in orthotropic material properties overall. The thickness of each composite layer is 0.12 mm and of each piezoceramic layer 0.24 mm. The structure is excited in exactly the same manner as in the first considered case – the electric voltage of 100 V supplied to the oppositely polarized piezolayers, which results in bending moments and structural deformation.

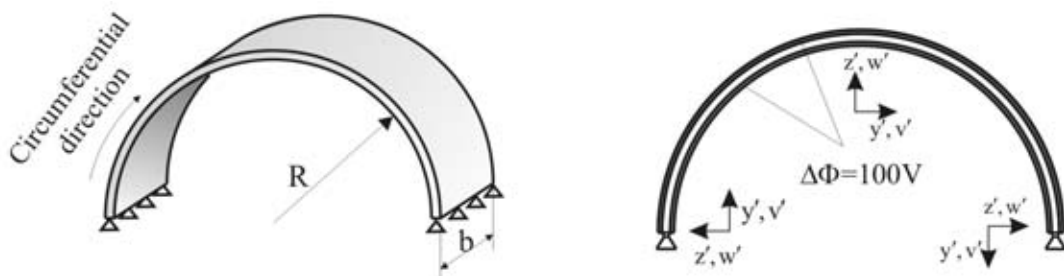


Fig. 6 Piezolaminated arch with boundary conditions

For the purpose of convergence analysis, the structure has been discretized with 3 FE meshes, each having four elements across the width, while the number of elements in the circumferential direction goes from 10, over 20, to 40, because the radial deflection of the width mid-line (w') along the circumference of the arch is the result of interest in this case. The results are given in the form of diagrams. Fig. 7 depicts the results for the *Semi-Loof* element, while Figs. 8 and 9 give the same for the *ACShell9* element with the full and reduced integration applied, respectively. It can be noticed that all three diagrams yield the same converged solution. Actually, further mesh refinement has been performed, but it has yielded a negligible difference in results (compared with the result for the mesh with 40 elements along the circumference) with both elements and those results are omitted here for the sake of brevity. The roughness of the result yielded by the *Semi-Loof* element for the mesh with 10 elements in circumferential direction is particularly remarkable. This is the consequence of the fact that it is an 8-node element (no full biquadratic shape functions applied), as opposed to the 9-node *ACShell9* element. The reduced integrated *ACShell9* element yields satisfactory results already with the roughest mesh considered. The results obtained for all three meshes with the under-integrated *ACShell9* element are close enough in Fig. 9 to make it difficult to differentiate the lines from each other. The lines obtained with the fully integrated *ACShell9* element using the meshes with 10 and 20 elements along the circumferential direction (Fig. 8) demonstrate a suboptimal convergence of the fully integrated element as a consequence of locking effects.

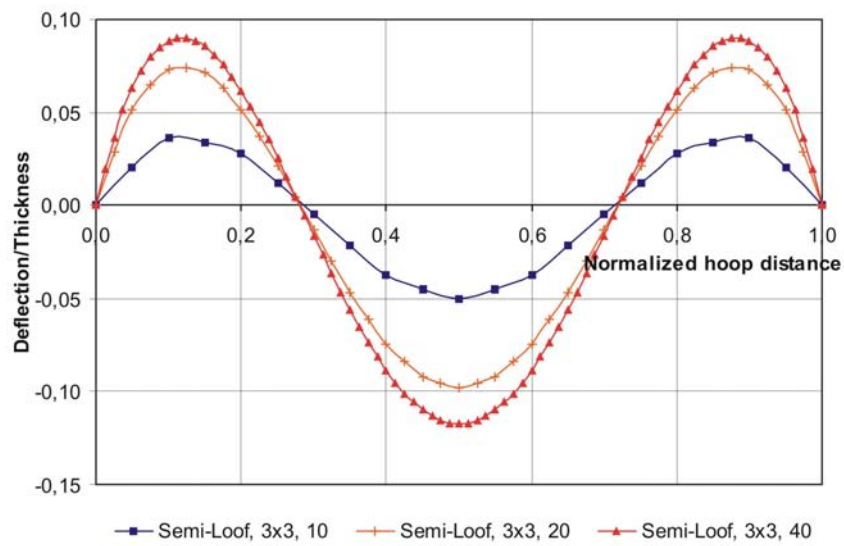


Fig. 7 Radial deflection of the cylindrical arch – results by the *Semi-Loof* element

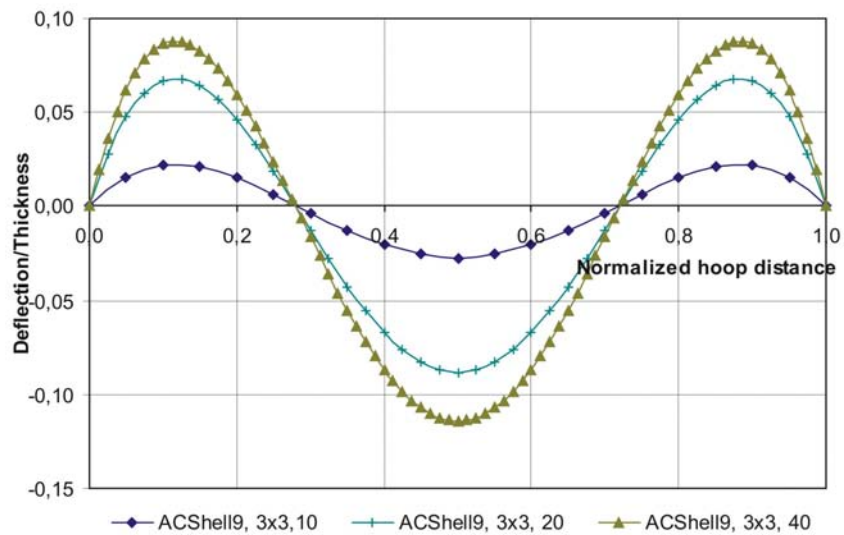


Fig. 8 Radial deflection of the cylindrical arch – results by the fully integrated *ACShell9* element

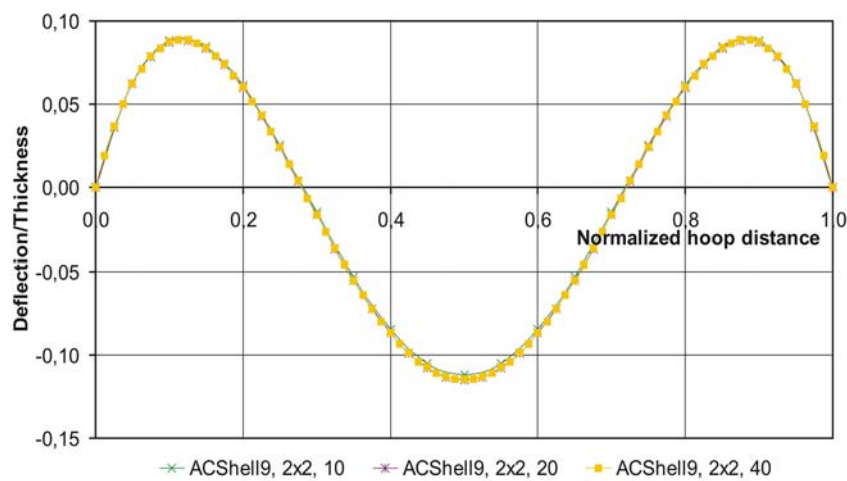


Fig. 9 Radial deflection of the cylindrical arch – results by the reduced integrated *ACShell9* element

5. Conclusions

Structural analysis requires reliable and accurate numerical tools. This is particularly emphasized with active structures characterized by two-way coupled-field problems. Numerical problems present in the solution for one of the fields are reflected in the solution for the other field as well, thus rendering the problem more complex and costly. In the framework of the FEM, the convergence of the obtained results with mesh refinement is a very important tool that assures the reliability of the results. The important conclusion of this paper is that a non-monotone convergence is a possibility in the FEM analysis of coupled-field problems. In the considered static analysis of piezoelectric active structures, it occurs as a consequence of the fact that both sides of the FEM equation are affected by mesh refinement, whereby they exhibit a different rate of convergence.

Another important conclusion is related to the rather fast rate of convergence of the under-integrated *ACShell9* element. It is a known fact that the reduced integration offers a remedy for locking effects for many different elements, but this technique is not a derivative of the variational approach (variational correctness not guaranteed), i.e. it is a kind of an *ad-hoc* method. One of the explanations for the success of the approach lies in the fact that the points of reduced integration are at the same time the Barlow points, i.e. the points that give the best estimates of strains/stresses for an element [1]. Hence, it is reasonable to expect that the parasitic strain and stress terms (which are the cause of locking effects) have the least influence on the accuracy of the obtained results when evaluated at those points.

Further work is supposed to provide an analysis of influence of mesh refinement onto the FE results convergence when sensor application of active elements is considered.

REFERENCES

- [1] Prathap, G., 1993, *The finite element method in structural mechanics*, Kluwer Academic Publishers, Netherlands.
- [2] Tzou, H. S. and Tseng, C. I., 1990, *Distributed piezoelectric sensor/actuator design for dynamic measurement/control of distributed parameter systems: a finite element approach*, Journal of Sound and Vibration, Vol. 38, pp. 17–34.
- [3] Zemčík, R., Rolfes, R., Rose, M., Tessler, J., 2006, *High-performance 4-node shell element with piezoelectric coupling*, Mechanics of Advanced Materials and Structures, Vol. 13, pp. 393–401.
- [4] Lammering, R., 1991, *The application of a finite shell element for composites containing piezo-electric polymers in vibration control*, Computers and Structures Vol. 41, pp. 1101–1109.
- [5] Marinkovic, D., Koeppe, H., Gabbert, U., 2006, *Numerically efficient finite element formulation for modeling active composite laminates*, Mechanics of Advanced Materials and Structures, Vol. 13, pp. 393–401.
- [6] Klinkel, S. and Wagner, W., 2006, *A geometrically non-linear piezoelectric solid shell element based on a mixed multi-field variational formulation*, International Journal for Numerical Methods in Engineering, Vol. 65, pp. 349–382.
- [7] Sze, K. Y. and Pan, Y. S., 1999, *Hybrid finite element models for piezoelectric materials*, Journal of Sound and Vibration, Vol. 226, No. 3, pp. 519–547.
- [8] Long, C. S., Loveday, P. W., Groenwold, A. A., 2006, *Planar four node piezoelectric elements with drilling degrees of freedom*, International Journal for Numerical Methods in Engineering, Vol. 65, pp. 1802–1830.
- [9] Liu, G. R., Dai, K. Y. and Nguyen, T. T., 2007, *Theoretical aspects of the smoothed finite element method (SFEM)*, International Journal for Numerical Methods in Engineering, Vol. 71, pp. 902–930.
- [10] Marinković, D., Marinković, Z., Petrović G., 2012, *On efficiency of a single-layer shell element for composite laminated structures*, Facta Universitatis, series Mechanical Engineering, Vol. 10, No. 2, pp. 105–112
- [11] Marinković, D., 2007, *A new finite composite shell element for piezoelectric active structures*, Ph.D. thesis, Otto-von-Guericke Universität Magdeburg, Fortschritt-Berichte VDI, Reihe 20: Rechnerunterstützte Verfahren, Nr. 406, VDI Verlag, Düsseldorf.

- [12] Marinković, D., Köppe, H., Gabbert U, 2007, *Accurate modeling of the electric field within piezoelectric layers for active composite structures*, Journal of Intelligent Material Systems and Structures, Vol. 18, No. 5, pp. 503-513
- [13] Marinković, D., Köppe, H., Gabbert, U, 2009, *Aspects of modeling piezoelectric active thin-walled structures*, Journal of Intelligent Material Systems and Structures, Vol. 20, No.15, pp. 1835-1844.
- [14] Ikeda T.1996, *Fundamentals of Piezoelectricity*, Oxford University Press Inc., New York
- [15] Marinković D., Nestorović T., Marinković Z., Trajkov M., 2012, *Modelling and Simulation of Piezoelectric Adaptive Structures*, Transactions of FAMENA, Vol. 36, No 1, pp. 25-34.
- [16] Nestorović, T., Shabadi, S., Marinković, D., Trajkov, M., 2013, *Modeling of piezoelectric smart structures by implementation of a user defined shell finite element*, Facta Universitatis, series Mechanical Engineering, Vol. 11, No. 1, pp. 1-12
- [17] Irons B. M., *The semiloof shell element*, in Ashwell D. G. and Gallagher R. H. (Eds.), 1976, *Finite elements for thin shells and curved membranes*, chapter 11, pp. 197-222, Wiley
- [18] Gabbert, U., Köppe, H., Seeger, F., Berger, H., 2002, *Modeling of smart composite shell structures*, Journal of Theoretical and Applied Mechanics, Vol. 3, Issue 40, pp. 575-593.

Submitted: 22.7.2013

Accepted: 22.11.2013

Dragan Marinković
Department of Structural Analysis, Berlin
Institute of Technology, Strasse des 17.
Juni 135, Berlin, Germany
Faculty of Mechanical Engineering,
University of Nis, A. Medvedeva 14, Nis,
Serbia
Manfred Zehn
Department of Structural Analysis, Berlin
Institute of Technology, Strasse des 17.
Juni 135, Berlin, Germany
Zoran Marinković
Faculty of Mechanical Engineering,
University of Nis, A. Medvedeva 14, Nis,
Serbia